



CrossMark  
click for updates

Cite this: *RSC Adv.*, 2017, 7, 3353

Received 28th November 2016  
 Accepted 22nd December 2016

DOI: 10.1039/c6ra27441b

[www.rsc.org/advances](http://www.rsc.org/advances)

# Hyperporphyrin effects extended into a J-aggregate supramolecular structure in water†

Adrián Zurita, Anna Duran, Josep M. Ribó, Zoubir El-Hachemi\* and Joaquim Crusats\*

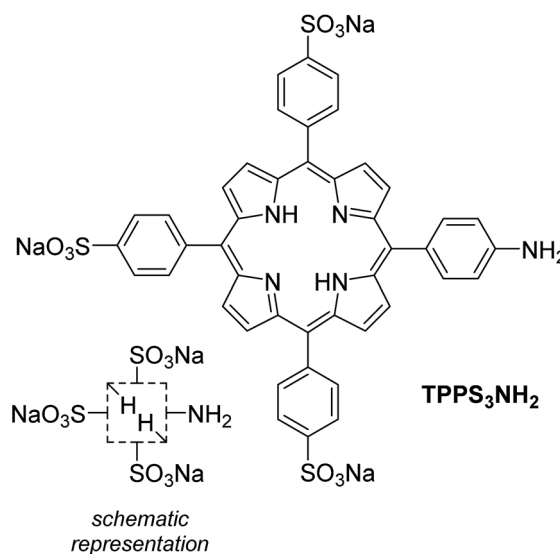
The relationship between the acid–base chemistry and the supramolecular behavior of 5-(4-aminophenyl)-10,15,20-tris(4-sulfonatophenyl) porphyrin in acidic water is reported. A new species exhibiting a prominently red-shifted Q-absorption band at 742 nm is described which is in accordance with a hyperporphyrin-type spectrum of a J-aggregate in water. UV-vis spectroscopy and peak force microscopy reveal that depending on the pH value of the medium the porphyrin self-assembles into two structurally different mesophases which can be reversibly interconverted at will.

Self-organized materials obtained from the self-assembly of monomers that form J-aggregates<sup>1</sup> arranged in a regular fashion are nowadays promising candidates with potential applications in energy and electron transfer processes in nanostructured materials. In this regard, supramolecular homoassociates of water-soluble porphyrins have received much attention.<sup>2</sup>

Inspired both by the hyperporphyrin aggregates described for the first time by Monsù Scolaro *et al.*<sup>3</sup> using hydroxy-substituted porphyrins and by the more recent report by Wamser *et al.*<sup>4</sup> on the acid–base chemistry of amino-substituted hyperporphyrins in organic media, we set forth to investigate if both approaches could converge using the water-soluble 5-(4-aminophenyl)-10,15,20-tris(4-sulfonatophenyl)porphyrin (TPPS<sub>3</sub>NH<sub>2</sub>, Scheme 1) as a suitable monomeric building block with the aim to compare its supramolecular behavior with that of the well-known 5,10,15,20-tetrakis(4-sulfonatophenyl) porphyrin (TPPS<sub>4</sub>).<sup>5</sup> The results of our investigation are presented in what follows.

The spectrophotometric titration<sup>6</sup> of TPPS<sub>3</sub>NH<sub>2</sub> (species of Fig. 1) could not be conveniently performed in buffered solutions at different pH values owing to an enhanced propensity of

this porphyrin to aggregate in solutions of high ionic strength (see below). Instead, a  $1.4 \times 10^{-6}$  M aqueous solution of the free base form was titrated with sulfuric acid without any interference from the presence of aggregated species (ESI<sup>†</sup>). In spite of sharp isosbestic points in the spectrophotometric titration (ESI<sup>†</sup>), only a rough average value for  $(pK_{a1} + pK_{a2})/2 = 5.06 \pm 0.02$  corresponding to the transition from the free base porphyrin to the diprotonated form (protonation at the inner pyrrolic nitrogen atoms, Fig. 1) could be measured. This was caused by the unusually high presence of the monoprotonated species<sup>7</sup> as a consequence of its stabilization originated by the electronic conjugation between the protonated central nitrogen atom the peripheral unprotonated amino group.<sup>4†</sup> However, although the presence of the lateral amino group does indeed seem to stabilize the monoprotonated form as reported,<sup>4</sup> it does not have a substantial effect on the basicity of the central



Scheme 1 Chemical structure of TPPS<sub>3</sub>NH<sub>2</sub> and its schematic representation used in this communication.

Departament de Química Inorgànica i Orgànica, Secció de Química Orgànica, Institut de Ciències del Cosmos (ICC), Universitat de Barcelona, Martí Franquès 1, 08028-Barcelona, Catalonia, Spain. E-mail: zelhachemi@ub.edu; j.crusats@ub.edu

† Electronic supplementary information (ESI) available: For materials and methods, synthetic procedures, HPLC analysis, acid–base titrations, aggregation studies and further PFM images. See DOI: 10.1039/c6ra27441b



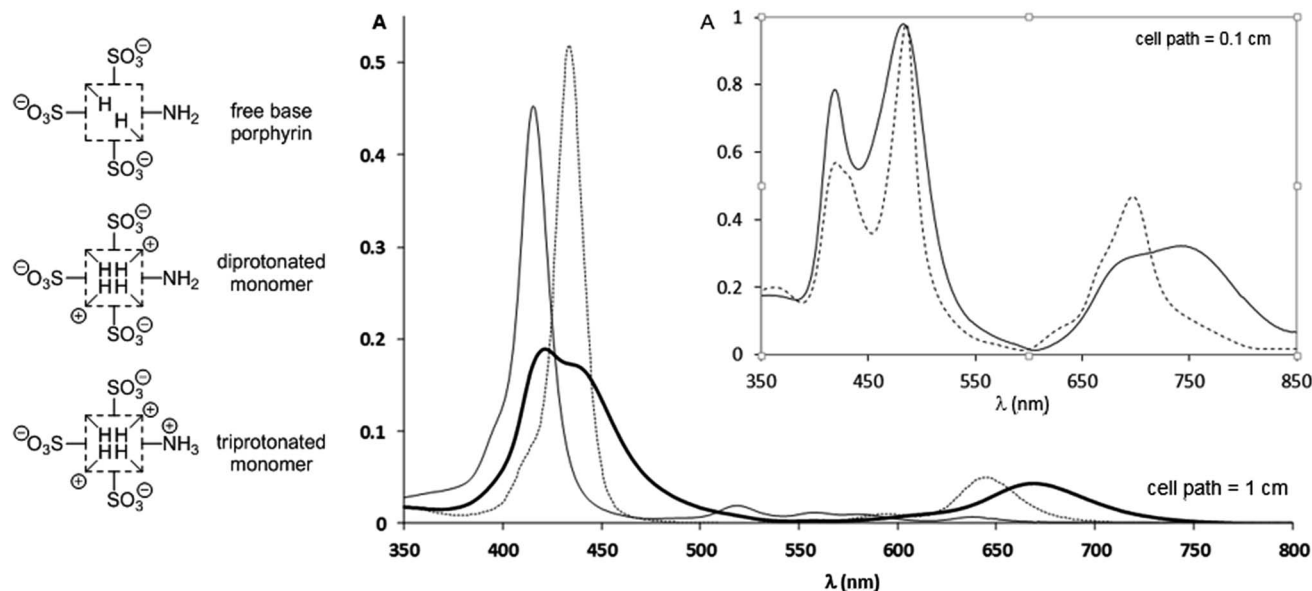


Fig. 1 UV-vis spectra of an aqueous  $1.40 \times 10^{-6}$  M solution of  $\text{TPPS}_3\text{NH}_2$  at different pH values ( $\text{H}_2\text{SO}_4$ ); continuous line: free base porphyrin monomer (pH = 7.0); bold line: the diprotonated monomer showing a hyperporphyrin-like spectrum (pH = 4.0); dotted line: triprotonated monomer (pH = 1.0). For the whole quantitative spectrophotometric titration of the porphyrin see the ESI.† Inset: supramolecular aggregates of the acidic forms of  $\text{TPPS}_3\text{NH}_2$  at different pH values; continuous line: a  $6.25 \times 10^{-6}$  M solution of  $\text{TPPS}_3\text{NH}_2$  in an aqueous buffer at pH = 4.0 (AcOH, AcONa 0.1 M) in which the aggregates of the diprotonated form predominate; dotted line: a  $1.47 \times 10^{-4}$  M solution of  $\text{TPPS}_3\text{NH}_2$  in aqueous HCl 0.1 M corresponding to the aggregates of the triprotonated zwitterionic form; the presence of residual monomeric units is evident from the shoulder at 433 nm.

core of the porphyrin ring in water.<sup>6</sup> It had already been unambiguously established that the inner pyrrolic nitrogen atoms of the macrocycle are more basic than the peripheral *meso*-4-aminophenyl group,<sup>4,8</sup> as we could corroborate during the titration of  $\text{TPPS}_3\text{NH}_2$ . Then, the  $\text{pK}_a$  value determined for the *meso*-anilinium cation was found to be:  $2.84 \pm 0.02$ , corresponding to a basicity more than two orders of magnitude lower than that of the central nitrogen atoms. As a consequence, solutions of the monomeric free-base, diprotonated, and triprotonated forms can all be adequately obtained so that their UV-vis spectra can be recorded as individual species (Fig. 1 and Table 1). The spectrum of the free base shows the expected absorption bands for a monosubstituted *meso*-4-aminophenylporphyrin.<sup>4</sup> Upon diprotonation of the inner nitrogen atoms a distinctive hyperporphyrin spectrum showing a split Soret band together with an unusually red-shifted Q-band is recorded, in accordance with the presence of the conjugated amino group.<sup>§</sup> Further protonation at the anilinic amino group results again in the typical absorption of the diacidic form of

a porphyrin protonated at both inner pyrrolic nitrogen atoms without any hyperporphyrin features in the spectrum.<sup>4</sup>

We then studied how the protonation state of the peripheral amino group affected the supramolecular behavior of the porphyrin and the electronic properties of the aggregates, in comparison to the currently well-known example of  $\text{TPPS}_4$ .<sup>5</sup> In relation to its tetrasulfonated counterpart,  $\text{TPPS}_3\text{NH}_2$  was found to have an increased propensity to homoassociate. Already at micromolar concentrations of the porphyrin, an order of magnitude lower than for  $\text{TPPS}_4$  (ESI<sup>†</sup>), aggregates could be detected by UV-vis spectroscopy, both in aqueous HCl 0.1 M (triprotonated form,  $-\text{NH}_3^+$ ) and in AcONa/AcOH 0.1 M buffer at pH = 4.0 (diprotonated form,  $-\text{NH}_2$ ). The UV-vis spectra of these aggregated species are presented on the inset of Fig. 1. The absorption spectrum of the aggregates of the triprotonated form [ $\lambda_{\text{max}}$ : 418 nm (H-agg.); 486 nm (J-agg.); 630<sub>sh</sub> nm; 666<sub>sh</sub> nm; 696 nm] is very much in line with the typical spectrum of those of  $\text{TPPS}_4$ ,<sup>5</sup> whereas, remarkably, the spectrum of the aggregates of the diprotonated form is clearly different. In this last case, although the maximum absorption of the J- and H-aggregates is almost unaltered (482 nm and 418 nm respectively), the absorption band of the J-aggregate is clearly wider and there is a most significant red-shift of a Q-band displaced to 742 nm. We attribute these changes in the J-aggregate absorption band to a hyperporphyrin effect caused by the electronic conjugation of the lone pair of the basic peripheral amino group<sup>3,4,9</sup> with the exciton band of the aggregate in analogy to what is observed for the corresponding diprotonated monomeric species. It is also significant that when the amino group is not protonated, even

Table 1 UV-vis absorption data [ $\lambda_{\text{max}}$  nm ( $\epsilon$ )] of the monomeric species of  $\text{TPPS}_3\text{NH}_2$  corresponding to the spectra in Fig. 1

Free base	Diprotonated form	Triprotonated form
415 (320.000)	423 (135.000)	434 (362.000)
519 (13.400)	436 (126.400)	593 (5.700)
560 (9.100)	610 <sub>sh</sub> (6.900)	645 (35.000)
579 (7.900)	669 (33.900)	
639 (4.100)		



at porphyrin concentrations as low as 10  $\mu\text{M}$  the presence of the monomer is not detected. Yet another difference between both types of aggregates is that the triprotonated form ( $-\text{NH}_3^+$ ) easily flocculates in the solution<sup>¶</sup> while the diprotonated form ( $-\text{NH}_2$ ) does not. In addition, both different aggregates ( $-\text{NH}_3^+/-\text{NH}_2$ ) can be reversibly interconverted merely by changing the pH of the solution once the mesophases are already formed (ESI<sup>†</sup>). Notice, however, that increasing the acidity of the medium to the extent that the sulfonato groups become protonated ( $\text{pH} \ll 0$ ) results, as expected, in the total disappearance of the aggregates.

The acid–base reversibility between both aggregates is also evidenced by peak force microscopy (PFM) measurements (Fig. 2). The mesophases deposited onto highly ordered pyrolytic graphite from a solution that shows an electronic spectrum with the hyperporphyrin absorption bands are very regular (aqueous HCl solution of  $\text{TPPS}_3\text{NH}_2$  at  $\text{pH} = 4.0$  obtained from the addition of a concentrated solution of the sodium salt of the free base porphyrin over the acid and left to aggregate for 24 hours leading to a solution with the expected UV-vis spectrum). In this case, wide plate-like structures consisting of monolayered 2-D aggregates appear on the graphite surface showing regions in which the flat structure is partially folded into a bilayer (3.7 nm of height) in analogy to what has been reported for other porphyrins bearing hydrophobic *meso*-substituents.<sup>10</sup> When an analogous solution of  $\text{TPPS}_3\text{NH}_2$  is similarly prepared but at lower pH values so that the amino group is protonated (aqueous HCl solution,  $\text{pH} = 1.3$ , with a UV-vis spectrum showing the predominance of the aggregates of the triprotonated form), only particles of different heights corresponding to multilayered structures can be detected (ESI<sup>†</sup>). The reversible interconversion between both types of aggregates was also corroborated by PFM: when a typical solution of  $\text{TPPS}_3\text{NH}_2$  at  $\text{pH} = 4.0$  showing the folded mesophases is further acidified to  $\text{pH} = 1.0$  with HCl, the folded structures do disappear, smaller aggregates form and flocculate, and again only irregularly shaped multilayered structures can be detected on the HOPG surface.

It is now rather well-established how the number and relative position of the anionic sulfonato groups in the *para*-position of the *meso*-phenyl groups of a protonated tetraphenylporphyrin

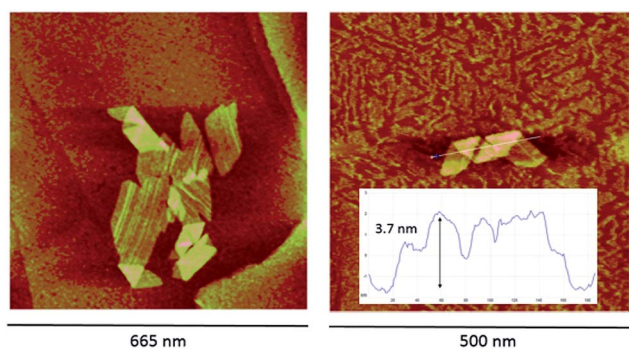
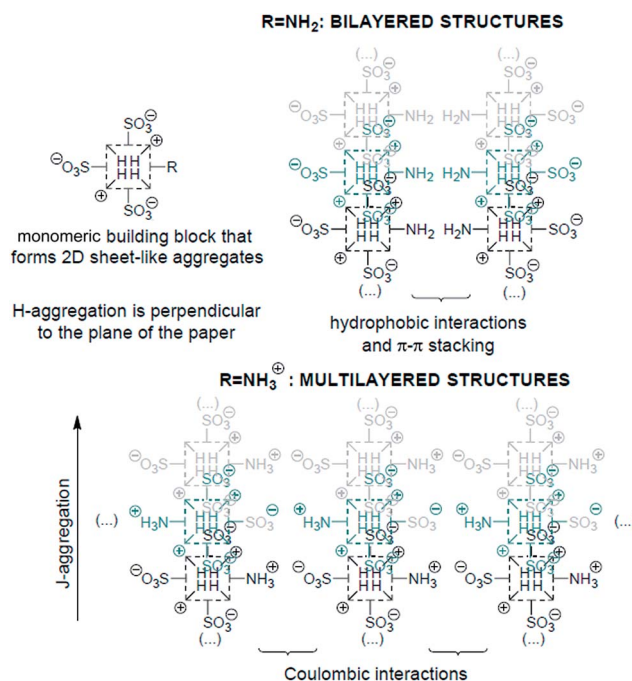


Fig. 2 PFM images (topographical map) of  $\text{TPPS}_3\text{NH}_2$  aggregates deposited on highly ordered pyrolytic graphite (HOPG) from an  $8.8 \times 10^{-5}$  M aqueous solution of the porphyrin at  $\text{pH} = 4.0$  (HCl). The inset shows the height analysis of the section of the spiral structure folded so as to form bilayered regions.

determine the shape of their self-assembled mesophases and, hence, some of their properties like chirality expression at the mesoscopic scale.<sup>11</sup> The results presented herein based on the tunable amino group (neutral vs. positively charged) at the periphery of the macrocycle show that not only the electronic properties of the J-aggregates can be effectively controlled at will, but also provide further evidence on how the supramolecular architectures of the aggregates can indeed be now predicted to a reasonable extent. The experimental results reported above can be reasonably interpreted as depicted in Scheme 2. Inasmuch as there are two opposite *meso*-4-sulfonatophenyl groups in  $\text{TPPS}_3\text{-NH}_2$ , the porphyrin is able to form aggregates *via* the same basic supramolecular pattern than  $\text{TPPS}_4$ .<sup>12</sup> In a first stage, oligomeric aggregates of the porphyrin further self-assemble into a two dimensional sheet-like structure consisting of J- and H-aggregates by the interaction of two opposite sulfonato groups of the same molecule with the positively charged central protonated pyrrolic nitrogen atoms of adjacent units, together with  $\pi$ - $\pi$  interactions and hydrophobic effects. Thereupon, the out-of-plane 5-(4-aminophenyl) and 15-(4-sulfonato-phenyl) groups can give rise to different stereoisomers of the porphyrin aggregates depending on the tacticity of these lateral groups in relation to the 2-D supramolecular sheet.<sup>13</sup> Depending on the protonation state of the amino group, the conspicuously different growth of the particles that leads to two distinctive mesophases can be rationalized as follows: when at lower pH values the peripheral amino groups are protonated, multilayered structures can easily grow owing to interlayer coulombic interactions (Scheme 2); this fact, together with the total charge compensation in the zwitterionic nature of the triprotonated



Scheme 2 Schematic representation of the different 3D packing motifs of the 2D sheet-like supramolecular structure of the  $\text{TPPS}_3\text{NH}_2$  aggregates depending on the protonation state of the peripheral amino group.



species accounts for the increased tendency of the porphyrin to flocculate. The bilayered structures, however, can be exclusively self-assembled when the amino groups are in their basic neutral form and a large enough region of the monolayer rearranges itself into an isotactic pattern with all the 4-aminophenyl groups on the same side of the 2-D structure. In this way, the supramolecular structure as a whole can gain additional thermodynamical stabilization owing to these supplementary interlayer hydrophobic and aromatic  $\pi$ - $\pi$  interactions provided by folding.

In summary, we report a new type of J-aggregate in water that exhibits a pH-activatable hyperporphyrin type absorption spectrum obtained from self-assembly of a *meso*-sulfonatophenyl-substituted porphyrin. In addition we have shown how the origin of the unusually red-shifted absorption Q-band of the J-aggregate is unambiguously correlated to the protonation state of the peripheral *p*-aminophenyl group of **TPPS<sub>3</sub>NH<sub>2</sub>**. In this way, the electronic characteristics of the J-aggregates can be reversibly tuned depending on the acidity of the media. This fundamental result may be of potential applicability for the design of novel pH-switchable self-assembled functional materials which optical properties in the near-infrared are based on a programmed response of the porphyrinic J-aggregates.

## Acknowledgements

Financial support from the Spanish Ministry of Economy and Competitiveness (MINECO), project CTQ2013-47401-C2-1-P and from Generalitat de Catalunya, project 2014SGR10, is gratefully acknowledged.

## Notes and references

‡ When the titrations of **TPPS<sub>3</sub>NH<sub>2</sub>** were performed with methanesulfonic acid in DMSO the results paralleled those reported for 5-(4-aminophenyl)-10,15,20-tris(4-carbomethoxyphenyl)porphyrin to the minor detail (ref. 4). However, when the titration was performed in water with sulfuric acid, although a significant presence of the porphyrin monocation could still be inferred, an increase of the intensity of the Soret band similar to that reported in ref. 4 was not observed (ESI†).

§ The split Soret band by 13 nm together with the red-shifted Q bands and the decreased  $\epsilon$  value depicted in Fig. 1 remain unaltered at the concentration limit of the UV-vis technique (**TPPS<sub>3</sub>NH<sub>2</sub>**  $\sim 10^{-7}$  M); in addition, we were unable to detect any resonance light scattering signal in this solution. The typical hyperporphyrin electronic spectra arise in transition metalloporphyrins as a consequence of the interaction between the porphyrin molecular orbitals and the p or d orbitals of the central metal atom (ref. 9). In the case of *meso*-aminophenyl substituted porphyrins with four hydrogen atoms in the core of the macrocycle, the same type of hyperporphyrin electronic spectra arise through the interaction of the peripheral *meso*-substituent with the molecular orbitals of the porphyrin ring. Further protonation of the amino group at the phenyl substituent results in the disappearance of the hyperporphyrin feature in the spectrum, as reported also herein (ref. 14).

¶ We have observed a similar behavior in all the members of a series of 5-(aryl- or heteroaryl)-10,15,20-tris(4-sulfonatophenyl)porphyrins in which there are three negatively charged peripheral sulfonate groups plus a fourth substituent bearing a positive charge. Unexpectedly, none of these porphyrins lead to solutions with detectable CD-signals during their supramolecular homoassociation process in acidic water, in contrast with what is commonly observed with **TPPS<sub>4</sub>** and its partially sulfonated counterparts. The results will be published elsewhere in due course.

- (a) *J-Aggregates*, ed. T. Kobayashi, World Scientific, Singapore, 1996; (b) F. Würthner, T. E. Kaiser and C. R. Saha-Möller, *Angew. Chem., Int. Ed.*, 2011, **50**, 3376.
- (a) R. F. Pasternack, P. R. Huber, P. Boyd, G. Engasser, L. Francesconi, E. Gibbs, P. Fasella, G. C. Venturo and L. D. C. Hinds, *J. Am. Chem. Soc.*, 1972, **94**, 4511; (b) O. Ohno, Y. Kaizu and J. Kobayashi, *J. Chem. Phys.*, 1993, **99**, 4128; (c) D. L. Akins, H.-R. Zhu and C. Guo, *J. Phys. Chem.*, 1994, **98**, 3612; (d) N. C. Maiti, M. Ravikanth, S. Mazumdar and N. Periasamy, *J. Phys. Chem.*, 1995, **99**, 17192; (e) R. Rubires, J. Crusats, Z. El-Hachemi, T. Jaramillo, M. Lopez, E. Valls, J.-A. Farrera and J. M. Ribó, *New J. Chem.*, 1999, **23**, 189; (f) N. Micali, F. Mallamace, A. Romeo, R. Purrello and L. Monsù Scolaro, *J. Phys. Chem. B*, 2000, **104**, 5897; (g) R. Rubires, J. A. Farrera and J. M. Ribó, *Chem.-Eur. J.*, 2001, **7**, 436; M. A. Castriciano, A. Romeo, V. Villari, N. Micali and L. Monsù Scolaro, *J. Phys. Chem. B*, 2003, **107**, 8765. (h) A. S. R. Koti, J. Taneja and N. Periasamy, *Chem. Phys. Lett.*, 2003, **375**, 171; (i) R. Rotomskis, R. Augulis, V. Snitka, R. Valiokas and B. Liedberg, *J. Phys. Chem. B*, 2004, **108**, 2833; (j) M. de Napoli, S. Nardis, R. Paolese, M. G. H. Vicente and R. Purrello, *J. Am. Chem. Soc.*, 2004, **126**, 5934; (k) A. L. Yeats, A. D. Schwab, B. Massare, D. E. Johnston, A. T. Johnson, J. C. De Paula and W. Smith, *J. Phys. Chem. C*, 2008, **112**, 2170; (l) L. Zhang and M. Liu, *J. Phys. Chem. B*, 2009, **113**, 14015; (m) M. A. Castriciano, A. Romeo, G. De Luca, V. Villari, L. M. Scolaro and N. Micali, *J. Am. Chem. Soc.*, 2011, **133**, 765; (n) A. Sorrenti, Z. El-Hachemi, J. Crusats and J. M. Ribó, *Chem. Commun.*, 2011, **47**, 8551.
- G. De Luca, A. Romeo and L. Monsù Scolaro, *J. Phys. Chem. B*, 2006, **110**, 14135.
- A. B. Rudine, B. D. DelFatti and C. Wamser, *J. Org. Chem.*, 2013, **78**, 6040.
- J. M. Ribó, J. Crusats, J.-A. Farrera and M. L. Valero, *Chem. Commun.*, 1994, **30**, 681.
- (a) P. Hambright, *Porphyrins and Metalloporphyrins*, ed. K. M. Smith, Elsevier Scientific Publishing Company, Amsterdam-Oxford-New York, 1975, pp. 235-238 and references cited therein; (b) T. P. G. Sutte, R. Rahimi, P. J. Hambright, C. Bommer, M. Kumar and P. Neta, *J. Chem. Soc., Faraday Trans.*, 1993, **85**, 495; (c) T. Gensch, C. Viappiani and S. E. Braslavsky, *J. Am. Chem. Soc.*, 1999, **121**, 10573.
- (a) F. Hibbert and K. P. P. Hunte, *J. Chem. Soc., Perkin Trans. 2*, 1977, 1624; (b) B. Cunderlikova, O. Kaalhus, R. Cunderlik, A. Mateasik, J. Moan and M. Kongshaug, *Photochem. Photobiol.*, 2004, **79**, 242.
- (a) E. C. A. Ojadi, H. Linschitz, M. Gouterman, R. I. Walter, J. S. Lindsey, R. W. Wagner, P. R. Droupadi and W. Wang, *J. Phys. Chem.*, 1993, **97**, 13192; (b) I. Hatay, B. Su, M. A. Méndez, C. Corminboeuf, T. Khoury, C. P. Gros, M. Bourdillon, M. Meyer, J. M. Barbe, M. Ersoz, S. Záliš, Z. Samec and H. H. Girault, *J. Am. Chem. Soc.*, 2010, **132**, 13733.
- M. Gouterman, *The Porphyrins*, ed. D. Dolphin, Academic Press, New York, 1978, vol. 3, p. 1.



- 10 C. Escudero, J. Crusats, I. Díez-Pérez, Z. El-Hachemi and J. M. Ribó, *Angew. Chem., Int. Ed.*, 2006, **45**, 8032.
- 11 (a) J. Crusats, J. Claret, I. Díez-Pérez, Z. El-Hachemi, H. García-Ortega, R. Rubires, F. Sagués and J. M. Ribó, *Chem. Commun.*, 2003, 1588; (b) A. Cabrer, J. M. Ribó, Z. El-Hachemi and J. Crusats, *J. Porphyrins Phthalocyanines*, 2015, **19**, 852.
- 12 (a) Z. El-Hachemi, C. Escudero, F. Acosta-Reyes, M. T. Casas, V. Altoe, S. Aloni, G. Oncins, A. Sorrenti, J. Crusats, J. L. Campos and J. M. Ribó, *J. Mater. Chem. C*, 2013, **1**, 3337; (b) M. J. Short, J. A. Berriman, C. Kübel, Z. El-Hachemi, J. V. Naubron and T. S. Balaban, *ChemPhysChem*, 2013, **14**, 3209; (c) J. V. Hollingsworth, A. J. Richard, M. G. H. Vicente and P. S. Russo, *Biomacromolecules*, 2012, **13**, 60; S. C. M. Gandini, E. L. Gelamo, R. Itri and M. Tabak, *Biophys. J.*, 2003, **85**, 1259.
- 13 Z. El-Hachemi, T. S. Balaban, J. L. Campos, S. Cespedes, J. Crusats, C. Escudero, C. S. Kamma-Lorger, J. Llorens, M. Malfois, G. R. Mitchell, A. P. Tojeira and J. M. Ribó, *Chem.–Eur. J.*, 2016, **22**, 9740.
- 14 M. Vitasovic, M. Gouterman and H. Linschitz, *J. Porphyrins Phthalocyanines*, 2011, **5**, 191.

